

Helicobacter pylori Resists the Antimicrobial Activity of Calprotectin via Lipid A Modification and Associated Biofilm Formation

Jennifer A. Gaddy,^{a,b} Jana N. Radin,^{b*} Thomas W. Cullen,^{e*} Walter J. Chazin,^{c,f} Eric P. Skaar,^{a,d} M. Stephen Trent,^g Holly M. S. Algood^{a,b,d}

Veterans Affairs Tennessee Valley Healthcare Services, Nashville, Tennessee, USA^a; Department of Medicine,^b Department of Biochemistry,^c and Department of Pathology, Microbiology and Immunology,^d Vanderbilt University, Nashville, Tennessee, USA; Institute of Cellular and Molecular Biology, University of Texas at Austin, Austin, Texas, USA^e; Center for Structural Biology, Vanderbilt University, Nashville, Tennessee, USA^f; Department of Infectious Diseases, University of Georgia, Athens, Georgia, USA^g

* Present address: Jana N. Radin, Department of Microbiology, University of Illinois, Urbana, Illinois, USA; Thomas W. Cullen, Novartis Institutes for BioMedical Research, Cambridge, Massachusetts, USA.

ABSTRACT *Helicobacter pylori* is one of several pathogens that persist within the host despite a robust immune response. *H. pylori* elicits a proinflammatory response from host epithelia, resulting in the recruitment of immune cells which manifests as gastritis. Relatively little is known about how *H. pylori* survives antimicrobials, including calprotectin (CP), which is present during the inflammatory response. The data presented here suggest that one way *H. pylori* survives the nutrient sequestration by CP is through alteration of its outer membrane. CP-treated *H. pylori* demonstrates increased bacterial fitness in response to further coculture with CP. Moreover, CP-treated *H. pylori* cultures form biofilms and demonstrate decreased cell surface hydrophobicity. In response to CP, the *H. pylori* Lpx lipid A biosynthetic enzymes are not fully functional. The lipid A molecules observed in *H. pylori* cultures treated with CP indicate that the LpxF, LpxL, and LpxR enzyme functions are perturbed. Transcriptional analysis of *lpxF*, *lpxL*, and *lpxR* indicates that metal restriction by CP does not control this pathway through transcriptional regulation. Analyses of *H. pylori* lpx mutants reveal that loss of LpxF and LpxL results in increased fitness, similar to what is observed in the presence of CP; moreover, these mutants have significantly increased biofilm formation and reduced cell surface hydrophobicity. Taken together, these results demonstrate a novel mechanism of *H. pylori* resistance to the antimicrobial activity of CP via lipid A modification strategies and resulting biofilm formation.

IMPORTANCE *Helicobacter pylori* evades recognition of the host's immune system by modifying the lipid A component of lipopolysaccharide. These results demonstrate for the first time that the lipid A modification pathway is influenced by the host's nutritional immune response. *H. pylori*'s exposure to the host Mn- and Zn-binding protein calprotectin perturbs the function of 3 enzymes involved in the lipid A modification pathway. Moreover, CP treatment of *H. pylori*, or mutants with an altered lipid A, exhibit increased bacterial fitness and increased biofilm formation. This suggests that *H. pylori* modifies its cell surface structure to survive under the stress imposed by the host immune response. These results provide new insights into the molecular mechanisms that influence the biofilm lifestyle and how endotoxin modification, which renders *H. pylori* resistant to cationic antimicrobial peptides, can be inactivated in response to sequestration of nutrient metals.

Received 7 August 2015 Accepted 2 November 2015 Published 8 December 2015

Citation Gaddy JA, Radin JN, Cullen TW, Chazin WJ, Skaar EP, Trent MS, Algood HMS. 2015. *Helicobacter pylori* resists the antimicrobial activity of calprotectin via lipid A modification and associated biofilm formation. mBio 6(6):e01349-15. doi:10.1128/mBio.01349-15.

Invited Editor Jason W. Rosch, St. Jude Children's Research Hospital **Editor** Larry S. McDaniel, University of Mississippi Medical Center

Copyright © 2015 Gaddy et al. This is an open-access article distributed under the terms of the [Creative Commons Attribution-Noncommercial-ShareAlike 3.0 Unported license](https://creativecommons.org/licenses/by-nc-sa/4.0/), which permits unrestricted noncommercial use, distribution, and reproduction in any medium, provided the original author and source are credited.

Address correspondence to Holly M. S. Algood, holly.m.algood@vanderbilt.edu.

Helicobacter pylori is a Gram-negative microaerophilic bacterium that infects about half of the world's population (1–3). Colonization with *H. pylori* results in both acute and chronic gastritis, and in a percentage of individuals it can lead to peptic ulcer disease or the development of stomach cancer (4, 5). As such, *H. pylori* has been classified by the World Health Organization as a class I carcinogen. The inflammatory response provoked by *H. pylori* includes infiltration of immune cells from both arms of the immune system into the lamina propria and gastric mucosa (6, 7). The inflammatory cascade is likely initiated by early interactions of *H. pylori* with the gastric epithelial cells and production of chemokines and cytokines, which elicit the recruitment of neutrophils and macrophages to the site of infection. Upon activation of

an adaptive immune response, a strong T cell-mediated response culminates in the production of proinflammatory cytokines, including gamma interferon (IFN- γ) and interleukin-17 (IL-17) (6, 8–18). This cytokine network results in further recruitment of innate immunity cells to the gastric mucosa, especially neutrophils. Despite this robust immune response, *H. pylori* persists within the gastric niche to promote a chronic infection for the duration of the host's life.

In order to survive the antimicrobial peptide response imposed by the vertebrate host, many Gram-negative bacteria utilize lipid A modifications (19–21). Bacteria accomplish this via several strategies, including adding positively charged moieties, such as phosphoethanolamine or L-4-aminoarabinose to the outer leaflet,

removing phosphate groups from the lipid A backbone, or changing the acylation pattern (22). Altering the bacterial surface charge reduces the binding affinity of cationic antimicrobial peptides (CAMPs) with the outer membrane. CAMPs are positively charged peptides produced by the host innate immune system that act by binding to bacteria through charged surface features, forming pores and thereby disrupting membrane integrity. For example, the enzyme responsible for dephosphorylation of the lipid A 4'-phosphate group in *H. pylori*, LpxF, is partially responsible for the resistance to the cationic antimicrobial peptide polymyxin (23). Thus, resistance to CAMPs via lipid A modification presents an important mechanism by which bacteria evade the host immune response.

An important antimicrobial factor that is also a component of the host innate immune system is calprotectin (CP). CP, a heterodimer of S100A8 and S100A9 subunits (also known as Mrp8/14, calgranulin A/B, and cystic fibrosis antigen), comprises about 50% of the neutrophil's cytoplasmic protein content and is a critical component of the host nutrient-withholding process termed nutritional immunity (24, 25). To prevent infection with pathogenic organisms, humans and other mammals restrict access to essential metals through nutritional immunity (26). It is clear that nutrient limitation by the host and nutrient acquisition by bacteria are crucial processes in the pathogenesis of infectious diseases. CP binds Mn and Zn with high affinity, which starves bacteria of these essential nutrient transition metals, creating a Mn- and Zn-limited environment. CP has two transition metal-binding sites: site 1 (S1; with six His) binds Mn and Zn, and site 2 (S2; with three His and three Asp) binds Zn only (27, 28). Previous reports have indicated that CP exhibits antimicrobial activity against numerous Gram-negative and Gram-positive pathogens (27, 29–36). Expression of CP subunits S100A8 and S100A9 increases in inflamed gastric tissues of *H. pylori*-infected individuals. Recent work has demonstrated that CP inhibits *H. pylori* growth and has the capacity to alter the activity of the major inflammatory virulence factor, the *cag* type IV secretion system (37). However, *H. pylori* persists in the gastric niche to promote chronic disease in the face of a robust immune response.

Work presented here demonstrates that *H. pylori* alters its lipid A molecules in response to CP, a phenotype that results in increased biofilm formation and increased bacterial fitness in the presence of CP. These results also demonstrate that CP-mediated nutrient restriction is responsible for the modification of lipid A, which mirrors modifications that exist in the context of LpxF inactivation, such as increased phosphate decoration of the outer membrane, increased bacterial fitness, and increased biofilm formation. Taken together, the data show that CP restricts the activity of LpxF (the 4'-phosphatase) and LpxL (an inner membrane acyltransferase) to promote resistance to CP by both inducing biofilm formation and outer membrane modification. Thus, this work indicates that *H. pylori* possesses strategies to circumvent the antimicrobial activity of CP and persist in its host.

RESULTS

***H. pylori* develops resistance to CP with exposure to subinhibitory doses.** Transition metals are essential micronutrients required by all living organisms. In response to infection, the vertebrate host produces antimicrobial proteins, such as calprotectin, lipocalin, lactoferrin, and transferrin, which sequester soluble metal ions (26, 31, 37, 38). In response to this nutritional immu-

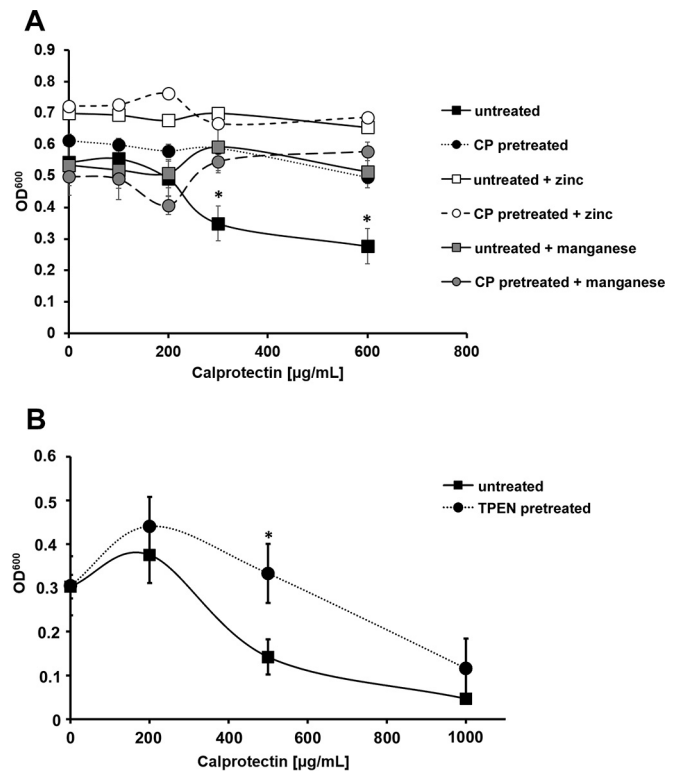


FIG 1 Exposure to subinhibitory levels of CP or TPEN confers increased resistance to the antimicrobial activity of CP. (A) Bacteria were cultured in medium alone (untreated) or medium plus subinhibitory concentrations of CP (CP pretreated), prior to culture in increasing concentrations of calprotectin in medium alone or medium supplemented with 100 μM Zn chloride (+ Zn) or 100 μM Mn chloride (+ Mn). (B) Bacteria were cultured in medium alone (untreated) or medium plus subinhibitory concentrations of TPEN (TPEN pretreated), prior to culture in increasing concentrations of calprotectin. Preexposure to zinc chelators (CP or TPEN) enhance bacterial fitness in the presence of increasing concentrations of CP. *, $P < 0.05$ via one-way ANOVA with Tukey's correction for multiple comparisons of the no-treatment group to the pretreatment with CP group. $n = 3$ biological replicates.

nity, bacteria alter their physiology and deploy elegant strategies to circumvent this antimicrobial response (39). To test the hypothesis that *H. pylori* responds to and alters its cellular biology to promote bacterial resistance or tolerance to the antimicrobial activity imposed by CP, *H. pylori* was cultured *in vitro* in the presence of 100 μg/ml of CP (a subinhibitory dose for bacterial growth), and pretreated *H. pylori* cells were then subcultured in increasing concentrations of CP. The bacterial fitness of CP-pretreated *H. pylori* and nonpretreated *H. pylori* was compared. CP pretreatment significantly increased bacterial fitness compared to samples that were untreated (Fig. 1A). The addition of exogenous Zn or Mn reversed the growth defect seen in bacterial cultures that were not pretreated with CP (Fig. 1A), but it did not alter the growth of bacteria pretreated with CP (Fig. 1A). To further investigate whether the increased bacterial fitness is due to Zn chelation, a synthetic metal chelator that preferentially binds Zn, *N,N,N',N'*-tetrakis(2-pyridylmethyl) ethylenediamine (TPEN), was tested for its ability to induce increased fitness in the presence of CP. *H. pylori* was grown in the presence of TPEN at concentrations below that necessary to inhibit growth (5 μM), and the abil-

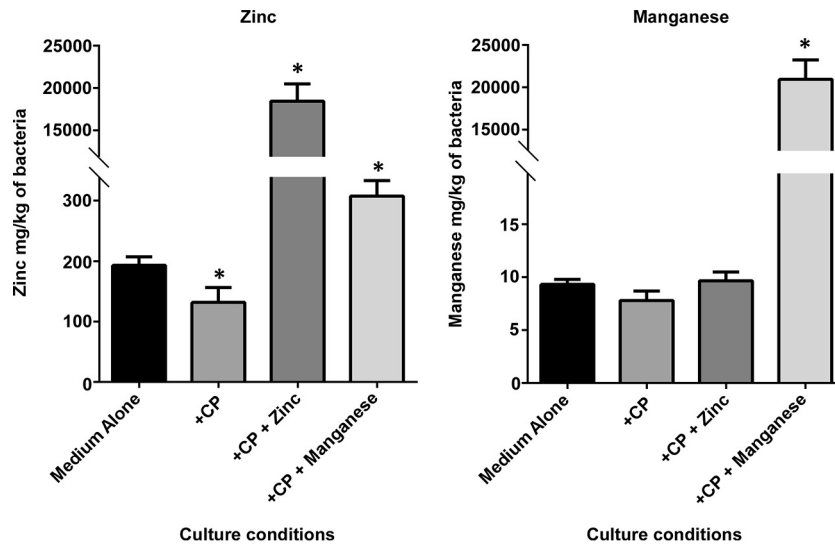


FIG 2 ICP-MS results for *H. pylori* bacteria exposed to CP. Bacteria were cultured in medium alone or medium supplemented with subinhibitory concentrations of CP, CP plus 100 μ M Zn chloride, or CP plus 100 μ M Mn chloride. Cell-associated levels of Zn (A) and Mn (B) (per kilogram of *H. pylori* cells) were determined by ICP-MS after *H. pylori* cells were cultured with and without CP and with and without supplementation with Zn or Mn chloride. *, $P < 0.05$, Student's t test with Welch's correction, compared to medium-alone control. $n = 3$ biological replicates.

ity to grow in the presence of increasing concentrations of CP was assessed. TPEN treatment of *H. pylori* led to increased resistance to CP (Fig. 1B). Together, these data indicate that exposure to CP under Zn-limiting conditions alters bacterial cell biology to confer increased resistance to the antimicrobial activity of CP. To investigate the impact of CP on metal restriction within *H. pylori*, inductively coupled plasma mass spectrometry (ICP-MS) was used. *H. pylori* was cultured with or without CP and with or without exogenous Zn or Mn supplementation. In cells grown in medium alone, Zn levels were 20-fold higher than Mn levels (average Zn level, 193 mg/kg; average Mn level, 9.33 mg/kg), demonstrating that cell-associated Mn levels are normally low within *H. pylori* in culture. The data indicated that the most profound effect of CP treatment of *H. pylori* was a 32% reduction in cell-associated Zn, a result that was statistically significant compared to cells grown in medium alone ($P = 0.0486$) (Fig. 2). Moreover, addition of exogenous Mn to CP-treated *H. pylori* increased cell-associated Zn levels. These data, combined with bacterial fitness data in the presence of CP and added transition metals, suggest that the effect of CP on *H. pylori* is largely through Zn restriction rather than Mn restriction.

Low-Zn conditions promote biofilm formation. During the course of investigating the growth phenotypes of *H. pylori* in response to CP, large clumps of bacterial cells and adherent bacterial cell structures on the sides of the culture tubes were observed in *H. pylori* cultures treated with subinhibitory concentrations of CP (100 μ g/ml). It was hypothesized that *H. pylori* will form biofilms in response to low nutrient metal conditions imposed by CP. To investigate this, *H. pylori* was cultured with and without CP in polystyrene tubes under static conditions for 24 to 48 h. Dense, confluent, macroscopic biofilms formed at the liquid-air interface when *H. pylori* was treated with CP, as demonstrated by staining of biofilms on culture tubes with crystal violet dye (Fig. 3A). Biofilms were quantified as previously described, using a spectrophotometry-based assay (40). The ratio of biofilm to biomass was enhanced in *H. pylori* cultures treated with CP and was reversed by the addition of ex-

ogenous Zn (Fig. 3A) and partially reversed with the addition of exogenous Mn (Fig. 3A). In addition to investigating the ability of wild-type (WT) CP to induce biofilm formation in *H. pylori* cultures, the effects of previously generated mutants of CP's metal-binding sites (Δ S1 and Δ S2 single mutants and Δ S1 Δ S2 double mutant) were investigated. Treatment of *H. pylori* with the Δ S1 Δ S2 double mutant of CP resulted in no increase in biofilm formation (Fig. 3B), indicating that metal-binding activity of this protein is critical for induction of this phenotype. When *H. pylori* was cultured with metal-binding site mutants of CP harboring inactivation of either S1 (Mn/Zn-binding site) or S2 (Zn-binding site) at high concentrations (600 μ g/ml), biofilm formation increased compared to that in untreated *H. pylori* (Fig. 3C and D). The observation that the Δ S1 mutant (Zn only) can still induce biofilm formation in *H. pylori* indicates that the Mn-binding activity of CP is dispensable for this phenotype. The final bacterial growth and the final biomass values from these experiments can be found in Table S1 in the supplemental material. To further investigate whether the biofilm phenotype is due to Zn chelation, a synthetic metal chelator that preferentially binds Zn, TPEN, was tested for its ability to induce biofilm formation. *H. pylori* was grown in the presence of TPEN at concentrations below that necessary to inhibit growth (5 μ M), and the ability to form macroscopic biofilms was assessed. TPEN treatment of *H. pylori* led to increased biofilm formation, and the addition of exogenous Zn reduced biofilm formation in TPEN-treated bacteria (Fig. 3B).

Because alteration in biofilm formation has previously been attributed to changes in cell surface hydrophobicity (41), the hypothesis that low Zn alters the hydrophobicity of the *H. pylori* cell surface was tested using the bacterial association to hydrocarbon (BATH) assay. *H. pylori* cells cultured in the presence of CP or TPEN had decreased cell surface hydrophobicity, as indicated by a decrease in *H. pylori* cells present in the xylene fraction compared to untreated *H. pylori* or bacteria treated with TPEN and exogenous Zn (Fig. 3A and B). Live-cell imaging of biofilms by confocal

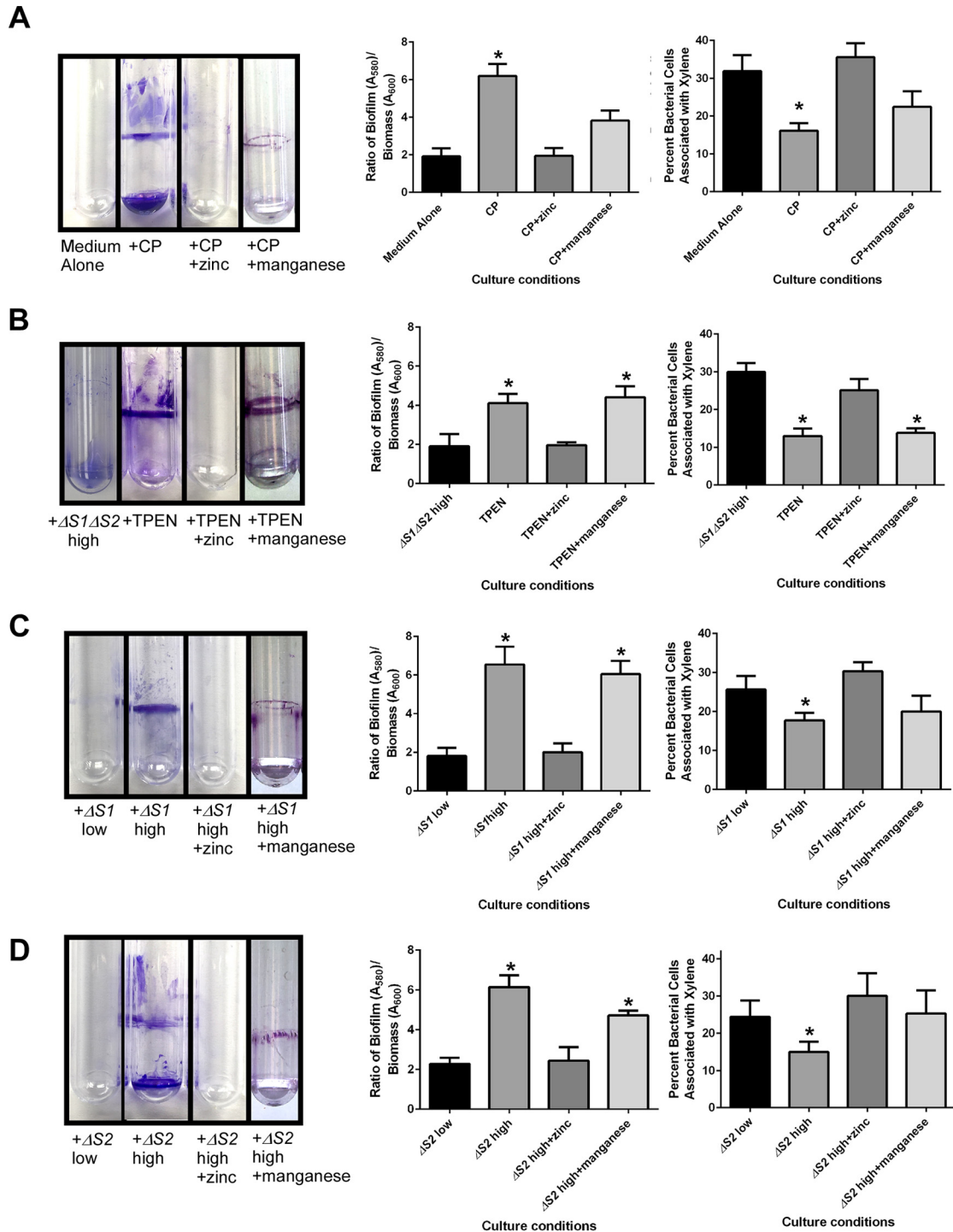


FIG 3 Subinhibitory concentrations of CP induce biofilm formation and changes in cell surface hydrophobicity of *H. pylori* cultures. Evaluation of *H. pylori* biofilm formation and cell surface hydrophobicity by cells cultured in medium alone, medium supplemented with 100 $\mu\text{g}/\text{ml}$ CP, medium supplemented with 100 $\mu\text{g}/\text{ml}$ CP plus 100 μM Zn chloride (CP + Zn), medium supplemented with 100 $\mu\text{g}/\text{ml}$ CP plus 100 μM Mn chloride (CP + Mn) (A); 600 $\mu\text{g}/\text{ml}$ $\Delta S1 \Delta S2$ double mutant, 5 μM synthetic Zn chelator (TPEN), or 5 μM TPEN plus 100 μM Zn chloride (TPEN + Zn), or 5 μM TPEN plus 100 μM Mn chloride (TPEN + Mn) (B); 100 $\mu\text{g}/\text{ml}$ $\Delta S1$ mutant ($\Delta S1$ Low), 600 $\mu\text{g}/\text{ml}$ $\Delta S1$ mutant ($\Delta S1$ High), 600 $\mu\text{g}/\text{ml}$ $\Delta S1$ mutant plus 100 μM Zn chloride ($\Delta S1$ High + Zn), or 600 $\mu\text{g}/\text{ml}$ $\Delta S1$ mutant plus 100 μM Mn chloride ($\Delta S1$ High + Mn) (C); 100 $\mu\text{g}/\text{ml}$ $\Delta S2$ mutant ($\Delta S2$ Low), 600 $\mu\text{g}/\text{ml}$ $\Delta S2$ mutant ($\Delta S2$ High), 600 $\mu\text{g}/\text{ml}$ $\Delta S2$ mutant plus 100 μM Zn chloride ($\Delta S2$ High + Zn), or 600 $\mu\text{g}/\text{ml}$ $\Delta S2$ mutant plus 100 μM Mn chloride ($\Delta S2$ High + Mn) (D). The photographic images depict *H. pylori* cultures stained with crystal violet after 48 h of growth. Bar graphs on the left represent mean biofilm-to-biomass ratios ($A_{580}/A_{600} \pm$ standard error of the mean). The total biofilm-to-biomass ratio was compared to that for medium alone (*, $P < 0.05$). The bar graphs on the right represent mean percentages of cell surface hydrophobicity (\pm standard errors of the means) as determined in a BATH assay. The cell surface hydrophobicity levels in the presence of CP were compared to those of cells grown in medium alone. Levels of significance were calculated based on growth via a one-way ANOVA with Tukey's correction for multiple comparisons, compared to results with medium alone. $n = 3$ to 5 biological replicates.

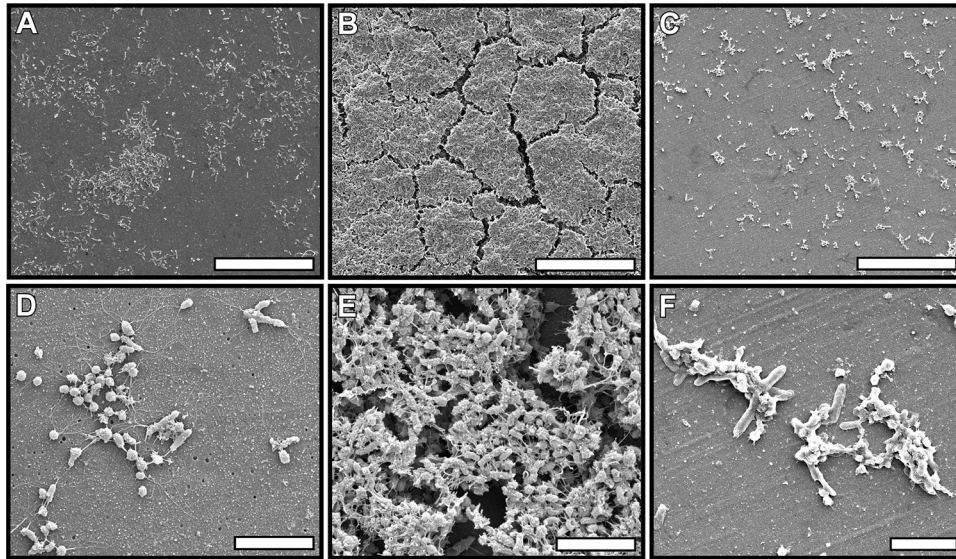


FIG 4 CP-dependent metal sequestration induces *H. pylori* biofilms. SEM analyses of biofilm formation in *H. pylori* cultures grown in medium alone (A and D), medium with 100 $\mu\text{g/ml}$ of CP (B and E), medium with 100 $\mu\text{g/ml}$ of CP supplemented with 100 μM Zn chloride (D and F). Original magnification, $\times 1,000$ (A to C) or $\times 7,000$ (D to F). Bars, 40 μm (A to C) or 5 μm (D to F). Micrographs are representative of three biological replicates.

laser scanning microscopy indicated that the tertiary structure of the CP-induced *H. pylori* biofilm was thicker than that of *H. pylori* grown in the absence of CP or in the presence of CP plus an exogenous source of nutrient Zn (see Fig. S1 in the supplemental material).

H. pylori biofilms induced by Zn sequestration were also visualized by field emission gun scanning electron microscopy (FEG-SEM). The microscopic view of these biofilms indicated that *H. pylori* cultures grown in the presence of CP or TPEN adhered to polystyrene and formed larger tertiary structures than did *H. pylori* cultures grown in medium alone, medium with exogenous Zn, or medium supplemented with a Zn chelator (CP or TPEN) and exogenous Zn (Fig. 4; see also Fig. S2 in the supplemental material). These biofilms had discrete multicellular aggregates of cells that appeared to intimately adhere to each other, with channels formed between these features. *H. pylori* can be described as a Gram-negative, spiral-shaped (S-shaped) or coccus-shaped bacterium. The three forms that have been reported are the viable and culturable spiral form, the viable but nonculturable (VBNC) coccoid form, and the nonviable degenerative form. The spiral shape is believed to enhance colonization of the gastric mucosa (42), and the helical shape was recently shown to be due to a Zn-dependent carboxypeptidase (43). The electron microscopy analyses revealed that both spiral and coccoid forms of *H. pylori* are present within the CP-induced biofilms, a result that is consistent with previous analyses of *H. pylori* biofilms (44). Therefore, these data suggest that low Zn availability imposed by CP induces an *H. pylori* biofilm.

Growth of *H. pylori* in the presence of CP inhibits the lipid A modification pathway. Since exposure to CP changed *H. pylori*'s surface properties and stimulated biofilm formation, we hypothesized that CP could alter the surface charge of the bacterium through modification of its lipopolysaccharide (LPS), a major surface determinant of charge (45, 46). To test this, lipid A purified from CP-treated *H. pylori* was evaluated by matrix-assisted laser desorption ionization–time of flight (MALDI-TOF) mass spec-

trometry analysis. Mass spectrometry analysis revealed two additional peaks present when *H. pylori* was treated with CP, which was unlike spectra from untreated *H. pylori* where one expected peak was evident (Fig. 5A). Adding back either Zn or Mn to *H. pylori* cultures treated with CP restored the production of wild-type lipid A, as did growth of *H. pylori* with a mutant of CP ($\Delta\text{S1 } \Delta\text{S2}$ double mutant) that does not bind Zn or Mn (Fig. 5A). Furthermore, the alteration of lipid A species was enriched in a dose-dependent manner with increasing concentrations of CP, as seen in the sample treated with 200 $\mu\text{g/ml}$ CP compared to the sample treated with 100 $\mu\text{g/ml}$ CP. These results indicated that Zn and/or Mn chelation by CP alters the biochemical machinery required for lipid A modification. Highlighted on the additional lipid A structures in Fig. 5B are the enzymes that could account for the structural features found on lipid A from the *H. pylori* cultures treated with CP. This result was specific to CP treatment of *H. pylori*, rather than a general stress response, because treatment of *H. pylori* with the synthetic Fe chelator 2,2'-dipyridyl did not alter the lipid A structure (data not shown) and is not involved in lipid A processing (23, 47–50). The affected pathway enzymes are an inner membrane acyltransferase, LpxL (Jhp0265), a 4'-phosphatase, LpxF (Jhp1486), and an outer membrane 3'-O-deacylase, LpxR (Jhp0634) (23). The predominant peak from the CP-treated *H. pylori* lipid A is at m/z 1546.8, consistent with the $[\text{M}-\text{H}]^-$ ion of the wild-type structure of *H. pylori* lipid A (predicted $[\text{M}-\text{H}]^-$ at m/z 1547.1) (Fig. 5B). The additional structure observed with an m/z of 1825.3 is consistent with a lipid A species that is penta-acylated with a phosphate group at the 4'-position and a phosphoethanolamine residue at the 1-position. The final peak on the spectrum from the CP-treated *H. pylori* with an m/z of 2092.5 is consistent with a lipid A species that is hexa-acylated with a phosphate group at the 4'-position and a phosphoethanolamine residue at the 1-position (predicted $[\text{M}-\text{H}]^-$ at m/z 2091.5). This final structure is the same lipid A species observed in an *H. pylori* ΔlpxF mutant, which is evidence that the lipid A modification pathway is an ordered process and the 3'-O-deacylase (LpxR) activity is de-

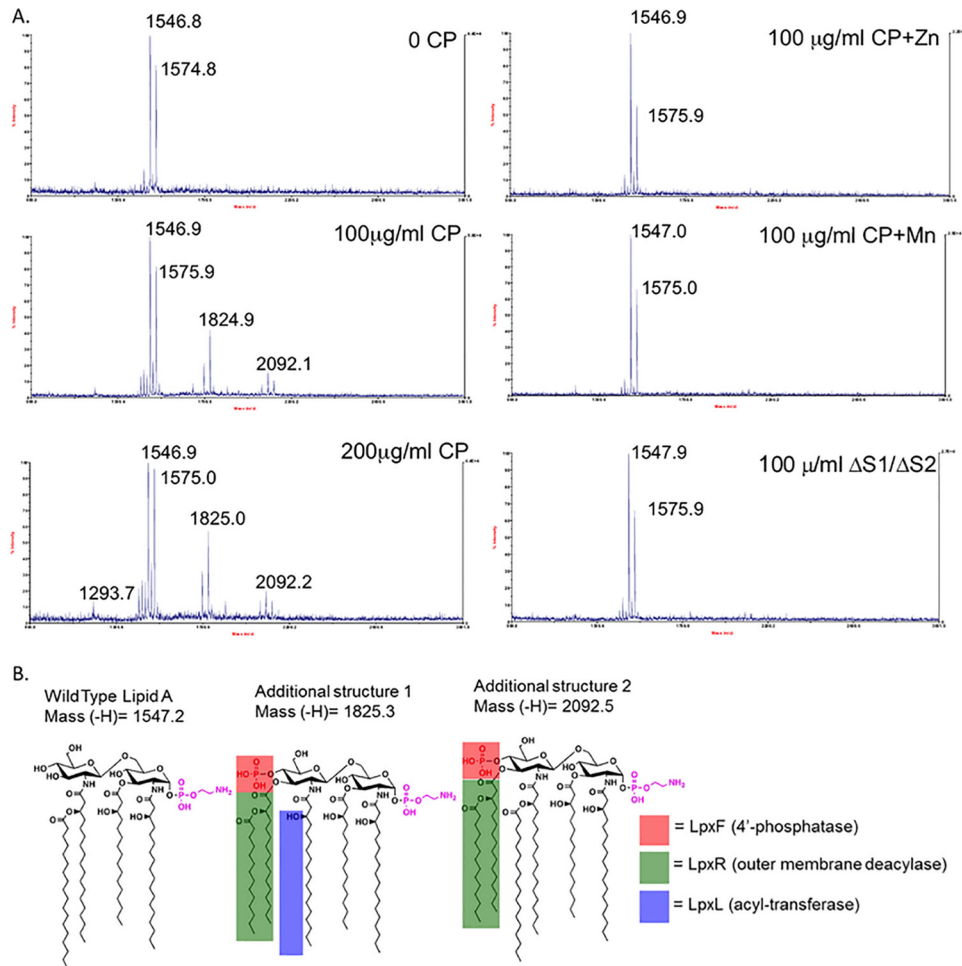


FIG 5 Growth of *H. pylori* in CP alters the *H. pylori* lipid A profile. Bacteria were cultured either in the absence of CP, with CP (100 $\mu\text{g/ml}$ or 200 $\mu\text{g/ml}$), with CP and medium supplemented with 100 μM Mn chloride or Zn chloride, or with the double site mutant of CP (ΔS1 ΔS2 at 100 $\mu\text{g/ml}$). (A) Mass spectrometry analyses of the lipid A species in response to CP-dependent metal sequestration. (B) Depictions of lipid A molecules identified by mass spectrometry in samples derived from *H. pylori* cultures treated with CP. The enzymes associated with modifying each moiety are highlighted (LpxF [red], LpxR [green], and LpxL [blue]). These results are representative of three separate biological replicates.

pendent on removal of the lipid A 4'-phosphate (23). Figure 5B depicts the altered lipid A molecules revealed by mass spectrometry analyses and the corresponding enzymes that are responsible for these modifications. This discovery that metal chelation alters the lipid A structure is highly significant, because changes in the lipid A structure have only been observed in *H. pylori* harboring mutational inactivation of genes encoding enzymes for the pathway. Therefore, CP is the first host factor identified which disrupts the synthesis of lipid A in *Epsilonproteobacteria*.

To determine whether the effect of CP on the lipid A modification pathway was a result of transcriptional control of *lpxF*, *lpxL*, and *lpxR*, transcriptional analysis of these genes was performed by real-time reverse transcription-PCR (RT-PCR). *H. pylori* was grown overnight either in medium alone, in the presence of 200 $\mu\text{g/ml}$ CP, or in the presence of 200 $\mu\text{g/ml}$ CP plus exogenous Zn, and transcript levels were determined using the relative gene expression method. Culture of *H. pylori* in the presence of CP did not affect transcription of *lpxF*, *lpxL*, or *lpxR* (see Fig. S3 in the supplemental material), suggesting that CP regulates this pathway through a posttranscriptional mechanism.

Inactivation of the 4'-phosphatase or the inner membrane acyltransferase alters surface charge and confers resistance to CP. Since the MALDI-TOF profiles of lipid A molecules formed in response to CP treatment are similar to those derived from *lpxF*, *lpxL*, or *lpxR* mutants, the next hypothesis tested was that inactivation of one or more of these genes could confer increased bacterial fitness in the presence of CP. Isogenic *lpxF*, *lpxL*, and *lpxR* mutants were generated in *H. pylori*, and growth curve analyses of these strains grown in increasing concentrations of CP were performed. It was previously reported that inactivation of LpxF, LpxL, and LpxR does not affect *in vitro* growth (23, 48). Inactivation of LpxF or LpxL in strain G27 was sufficient to increase bacterial fitness in the presence of 500 $\mu\text{g/ml}$ CP by more than 50% (Fig. 6), further supporting the hypothesis that lipid A modification can lead to resistance or tolerance to the antimicrobial activity of CP.

To determine how LpxF, LpxL, or LpxR contributes to bacterial surface charge and biofilm formation, the ability of these strains to form biofilm and associate with hydrocarbons was assayed through a BATH assay in both strains G27 and 7.13. All of

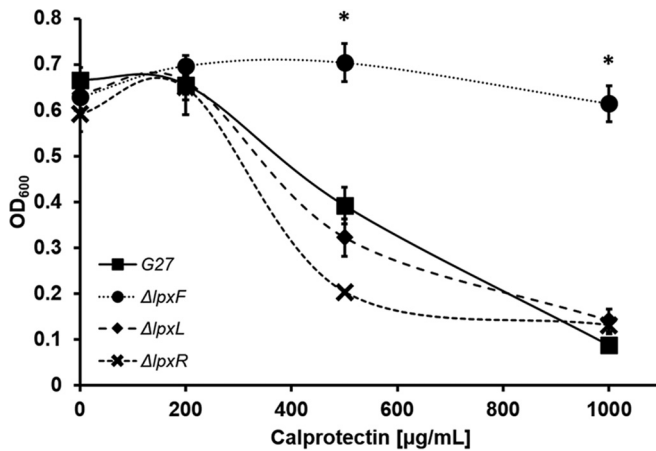


FIG 6 LpxF inactivation leads to increased bacterial fitness in the presence of CP. Spectrophotometric analysis of bacterial growth of *H. pylori* and *H. pylori* mutants was performed after culture with increasing concentrations of CP. Strains included WT *H. pylori* strain G27 and the $\Delta lpxF$ isogenic derivative, $\Delta lpxL$ isogenic derivative, and $\Delta lpxR$ isogenic derivative. One-way ANOVA with Tukey's correction for multiple comparisons was performed. ***, $P < 0.001$ for the $\Delta lpxF$ isogenic derivative compared to WT bacteria grown in the presence of 500 $\mu\text{g/ml}$ or 1,000 $\mu\text{g/ml}$ CP, or for the $\Delta lpxL$ isogenic derivative compared to WT in the presence of CP at 500 $\mu\text{g/ml}$. $n = 3$ biological replicates.

the isogenic mutants formed biofilms with a tertiary structure, based on macroscopic analysis and the ratio of biofilm to biomass (Fig. 7A; see also Fig. S4 in the supplemental material). The BATH assay analyses revealed that *lpxF* or *lpxL* inactivation is sufficient to promote the decreased bacterial cell surface hydrophobicity that is associated with the increased biofilm phenotype observed with CP treatment (Fig. 7A; see also Fig. S4). While *H. pylori* $\Delta lpxR$ forms a modest biofilm, it does not exhibit a decreased cell surface hydrophobicity, as seen in *H. pylori* $\Delta lpxF$ and *H. pylori* $\Delta lpxL$. This may explain why *H. pylori* $\Delta lpxR$, which may still have some positive charges on its cell surface, is still sensitive to CP, while *H. pylori* $\Delta lpxF$ and *H. pylori* $\Delta lpxL$ exhibit increased resistance to CP. To determine if chelation of Zn by CP or TPEN could enhance the biofilm formation further in these lipid A modification mutants, WT *H. pylori* and its *lpxF*, *lpxL*, and *lpxR* mutants were cultured with subinhibitory doses of CP or TPEN. Sequestration of Zn by either mechanism did not further enhance biofilm formation or modify cell surface hydrophobicity in *H. pylori* strains with lipid A modifications (Fig. 7B; see also Fig. S4). Also, the addition of both a Zn chelator and an exogenous source of nutrient Zn or Mn did not abolish biofilm formation by the *lpxF* isogenic derivative (Fig. 7C and D; see also Fig. S4), indicating that the inactivation of *lpxF* is sufficient to induce biofilm formation regardless of Zn availability.

Microscopically, the biofilms formed by *lpxF*, *lpxL*, and *lpxR* mutants were different from those formed by treating *H. pylori* with CP. The *H. pylori* $\Delta lpxF$ and the *H. pylori* $\Delta lpxL$ mutant formed more robust biofilms than the *H. pylori* $\Delta lpxR$ strain (Fig. 7). While isogenic derivatives lacking expression of LpxF, LpxL, or LpxR formed biofilms with similar tertiary structures to those formed by WT *H. pylori* exposed to CP (Fig. 4), CP-induced biofilms differed from the biofilms formed by $\Delta lpxF$, $\Delta lpxL$, and $\Delta lpxR$ mutants because they exhibited increased extracellular matrix and an increased incidence of coccoid cells (Fig. 4 and 8). This

result was likely due to the pleiotropic effects of CP treatment, which can affect multiple cellular responses in addition to the Lpx pathway. The $\Delta lpxF$ mutant displayed a confluent mat of cells with a few multicellular aggregates (Fig. 8). The $\Delta lpxL$ and $\Delta lpxR$ mutants had multicellular aggregates with less-developed tertiary architectures than CP-treated cells.

DISCUSSION

In an effort to suppress microbial outgrowth, the host sequesters essential nutrients in a process termed nutritional immunity. An antimicrobial protein associated with nutritional immunity and deposited at the sites of infection by neutrophils is CP. CP has antibacterial, antifungal, and immune-modulating effects that are dependent on its transition metal-binding capacity within two independent binding sites that have been shown to bind Mn and Zn with high affinity (28, 51). Because CP is present at high levels during immune responses to invading pathogens when neutrophils are present, understanding the effects of transition metal binding by CP on pathogen-associated molecular patterns, biofilm formation, and bacterial fitness will have broad implications.

In addition to inhibiting *H. pylori* growth *in vitro* and modulating function of the *H. pylori* cytotoxin type IV secretion system (37), in this study, the data demonstrated that exposure to subinhibitory concentrations of CP induces increased bacterial fitness in increasing concentrations of CP, changes *H. pylori*'s outer membrane structures, and produces a mixed species of lipid A (Fig. 5), affecting hydrophobicity and biofilm formation (see the model in Fig. 9). In these studies, the dominant lipid A structure is still WT, suggesting modification of lipid A does not have to completely inactivate the *lpx* genes to see these effects. Previous work indicated that genetic inactivation of LpxF in *H. pylori* leads to the inability to colonize female C57BL/6 mice, suggesting that early establishment of infection requires LpxF (23). However, the current data suggest that partial inactivation of LpxF by Zn sequestration after the establishment of colonization and the development of inflammation may lead to increased bacterial fitness and persistence. This discovery that metal chelation alters the lipid A structure is highly significant, because changes in the lipid A structures observed here in *H. pylori* cultures under Zn-limiting conditions have only been observed in *H. pylori* cells harboring mutations that inactivate genes encoding enzymes for the pathway. Therefore, CP is the first host factor identified that disrupts the biosynthetic genes involved in synthesis of lipid A. Importantly, these findings suggest that additional lipid A species may be found when neutrophils are responding to infection and depositing CP at the site of inflammation. Recent studies have indicated that lipid A modification enzymes, including LpxF, are highly prevalent in many gut-associated microbes (52), suggesting that CP could have a much broader role in shaping the microbial ecology within the human body in both commensal and pathogen bacteria alike. Levels of CP, and therefore its effects on bacteria, will differ during these infections, depending on the level and type of inflammation in the area. Proinflammatory cytokines such as IL-17a and IL-22 affect CP expression by epithelial cells, and the number of neutrophils in the area greatly influences the amount of CP in the tissue. Levels of CP used for the studies reported here could indeed be physiological. Concentrations of calprotectin in tissue have been reported to be as high as 20 mg/ml in response to bacterial infections (53).

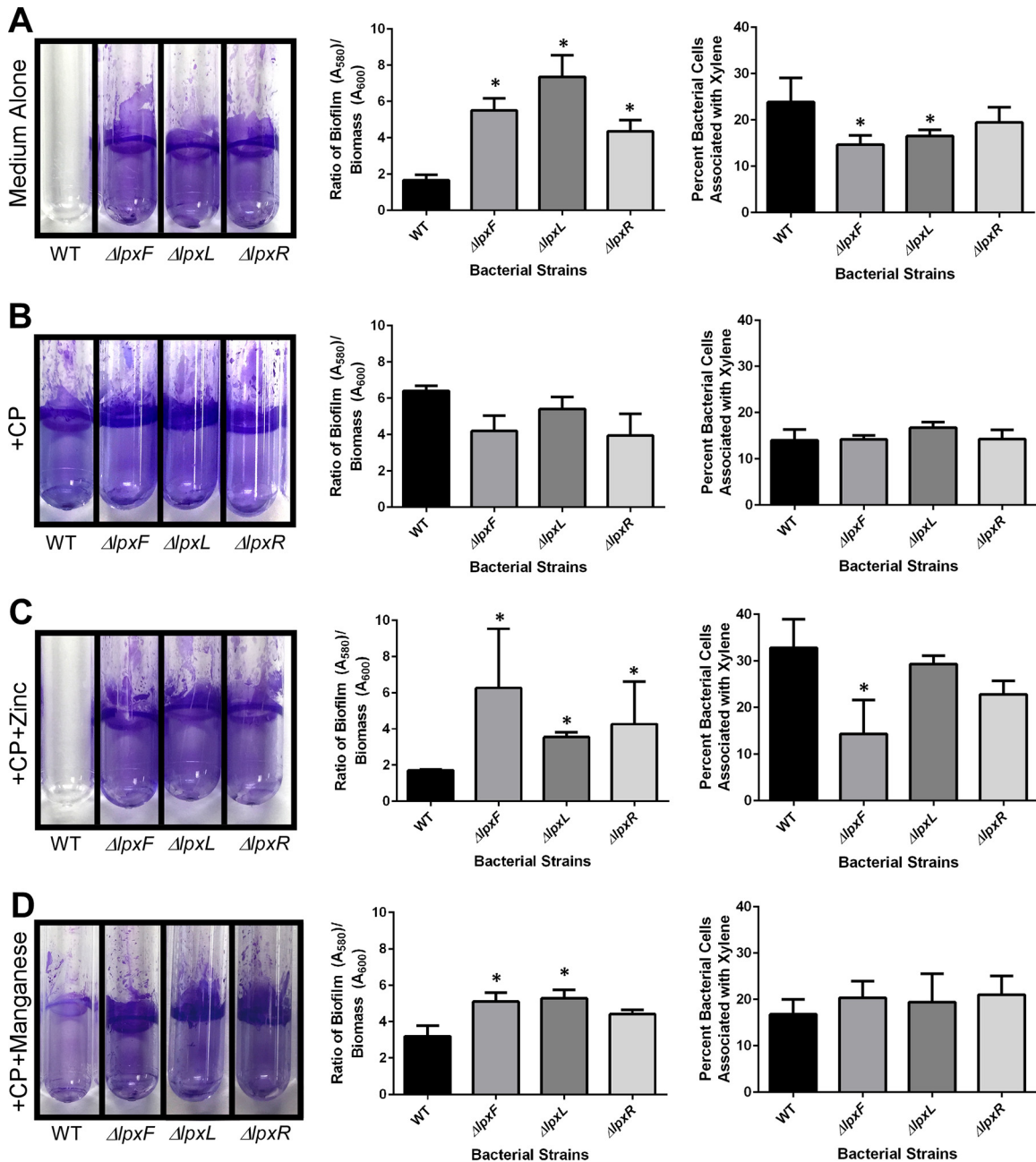


FIG 7 Changes in lipid A modification enzymes lead to increased biofilm formation and decreased cell hydrophobicity. Macroscopic evaluation of biofilm formation was performed on static *H. pylori* cultures stained with crystal violet. Photographic images of biofilm formation of *H. pylori* strain G27 and isogenic mutants of *lpxF*, *lpxL*, and *lpxR* in the absence of CP in medium alone (A), in the presence of 100 $\mu\text{g}/\text{ml}$ CP (B), in the presence of CP with medium supplemented with 100 μM Zn chloride (C), and in the presence of CP with medium supplemented with 100 μM Mn chloride (D). Quantification of the total biofilm-to-biomass ratio was calculated via a colorimetric assay and is presented in the bar graph on the left (A_{580}/A_{600}) \pm the standard errors of the means. Cell surface hydrophobicity was determined in a BATH assay and is presented in the graphs on the right (mean percentages of cell surface hydrophobicity \pm standard errors of the means). Levels of significance were calculated based on growth, using a one-way ANOVA with Tukey's correction for multiple comparisons. *, $P < 0.05$ compared to WT bacteria. $n = 3$ biological replicates.

The data presented in this study suggest that one way *H. pylori* may survive the stress imposed by the host immune system is through outer membrane endotoxin modification and associated biofilm formation. Modifications of the lipid A molecules within the outer membrane, imposed either by nutrient metal sequestration (through treating *H. pylori* with CP) or through mutations of

the Lpx machinery (especially LpxF) involved in lipid A synthesis, led to increased *H. pylori* fitness, biofilm formation, and decreased cell surface hydrophobicity *in vitro*. Interestingly, in the *H. pylori* *lpxL* mutant, when exogenous Zn was added back to the growth medium, there was a reduction in biofilm formation, suggesting that LpxF activity may be increased. Lipid A modifications in

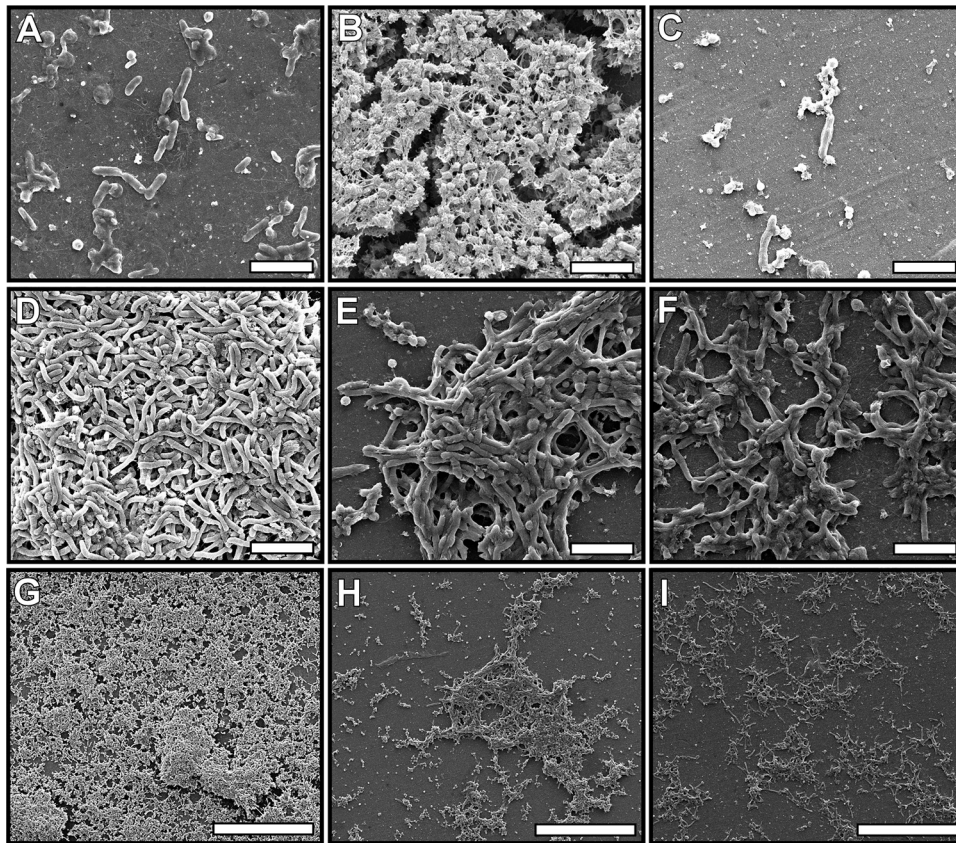


FIG 8 *H. pylori* cultures form biofilms with loss-of-function mutations in *lpxF*, *lpxL*, and *lpxR*. (A to C) High-resolution FEG-SEM analysis images of WT *H. pylori* strain G27 (A), WT *H. pylori* strain G27 exposed to CP (B), or *H. pylori* treated with CP plus 100 μM Zn chloride (C). (D to F) *H. pylori* ΔlpxF strain (D), *H. pylori* ΔlpxL (E), and *H. pylori* ΔlpxR isogenic mutants (F) grown in medium alone on plastic substrates. Original magnification, $\times 5,000$. Bars, 5 μm . (G to I) Images of FEG-SEM analysis of *H. pylori* ΔlpxF (G), *H. pylori* ΔlpxL (H), and *H. pylori* ΔlpxR (I) isogenic mutant strains. Original magnification, $\times 1,000$. Bars, 40 μm . Micrographs are representative of 3 biological replicates.

Gram-negative bacteria can lead to changes in biofilm formation in pathogens such as *E. coli* and *Pseudomonas aeruginosa* and the plant symbiont *Rhizobium leguminosarum* bv. *viciae* (51, 54, 55). Lipid A biosynthesis pathways have been linked to Zn availability, and several enzymes involved in these pathways are metal dependent. For example, the first committed step of lipid A biosynthesis in most Gram-negative bacteria is catalyzed by a conserved UDP-3-O-[(*R*)-3-hydroxymyristoyl]-*N*-acetylglucosamine deacetylase, a Zn-dependent deacetylase also known as LpxC (56–59). Moreover, in *Pseudomonas aeruginosa*, activation of the response regulator ColR specifically induces phosphoethanolamine addition to lipid A when Zn is present (60), suggesting that Zn can regulate lipid A modifications in other Gram-negative species at the transcriptional level. The data presented here demonstrate that a host protein can trigger these events in *H. pylori* through production of CP, which inhibits *H. pylori*'s lipid A modification pathway. While the crystal structure of *Salmonella enterica* serovar Typhimurium LpxR contains a Zn/Ca-binding site, it is Ca binding which supports the enzymatic activity of LpxR (61, 62). These observations and the data presented in this study suggest that CP inactivates these proteins by sequestering essential metals. Thus, our results indicate that CP-dependent chelation of nutrient metals leads to increased biofilm formation *in vitro* and that this is due to alterations in the lipid A modification pathway and

concomitant changes in characteristics of the cell surface. This could have broad implications in other Gram-negative bacterial species for which biofilm formation is a key virulence determinant.

Within chronic bacterial infections, the invading prokaryotes often persist in tissues in a biofilm state (63). A biofilm is a single- or multispecies community of organisms, typically attached to an abiotic or biotic surface in an architectural structure of cells that exist in a self-secreted matrix. This matrix is comprised of hydrated polysaccharides, secreted proteins, glycopeptides, extracellular DNA, and lipids (64). The presence of biofilm-associated extracellular matrix is well established in the literature for diverse bacterial pathogens such as *Staphylococcus epidermidis*, *Vibrio cholerae*, *Yersinia pestis*, *P. aeruginosa*, and *Listeria monocytogenes* among others (65–68). *H. pylori* biofilm extracellular matrices have been shown to contain proteomannans, extracellular DNA, and outer membrane vesicles (69–71). CP- or TPEN-induced biofilms differ from the biofilms formed by ΔlpxF , ΔlpxL , and ΔlpxR mutants because CP-induced biofilms exhibit increased extracellular matrix compared to Lpx pathway mutants. This result is likely due to the pleiotropic effects of CP or TPEN treatment, which could affect multiple cellular responses in addition to the Lpx pathway. On the other hand, the available data do not allow us

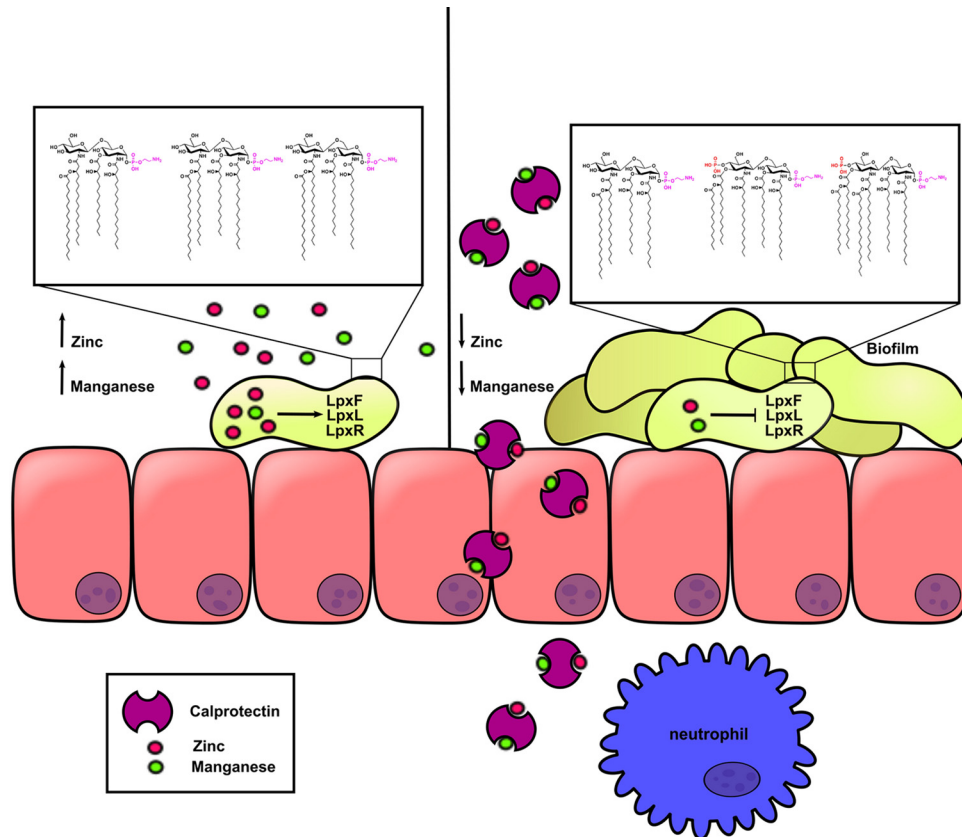


FIG 9 Model of *H. pylori* lipid modification and biofilm formation as a consequence of the Zn sequestration imposed by calprotectin. Under Zn-replete conditions, *H. pylori* cytoplasmic zinc levels are high and LpxF, LpxL, and LpxR remain active, leading to wild-type lipid A production. Calprotectin, which is deposited at the site of infection by innate immune cells, decreases cytoplasmic Zn levels, resulting in decreased LpxF, LpxL, and LpxR activity. This leads to production of alternative lipid A species, enhanced biofilm formation, and increased bacterial fitness and replication in the presence of calprotectin.

to rule out that biofilm formation and cell surface hydrophobicity are secondary effects.

Biofilms are characterized by increased resistance to antibiotics and antimicrobials (up to 1,000-fold) due to the physiological properties of the community structure (63, 72). Frequently, exposure to antimicrobial molecules induces biofilm formation in a variety of pathogens, including *Staphylococcus aureus*, *Streptococcus mutans*, and *P. aeruginosa* (73–75). Interestingly, a correlation exists between increased calprotectin expression and concomitant increases in biofilm formation with the dental pathogen *S. mutans* (76). Similarly, exposure to subinhibitory concentrations of amoxicillin and clarithromycin can increase *H. pylori* biofilm formation (77). While *H. pylori* biofilms have been previously observed via scanning electron microscopy, here we found that a host protein can induce this tertiary biofilm structure and that the structure correlates with changes in the lipid A biosynthesis pathway. CP-induced biofilm formation may protect *H. pylori* from a constantly changing environment within the host or in the environment, making these structures important for pathophysiology as well as resistance to both antimicrobial therapeutics and clearance by the immune system (44).

Our results combined with previously published work (37) reveal that *H. pylori* responds to the presence of CP (or TPEN) by altering its repertoire of toxins. Zn sequestration modulates the function of the *cag*-T4SS pili responsible for secreting the cytotoxin CagA (37) and the endotoxin-associated lipid A modifica-

tion pathway, cell surface hydrophobicity, and bacterial fitness. Such changes in bacterial cell biology may augment bacterial survival during exposure to inflammation-associated antimicrobials. These insights suggest a potential target and a new strategy for antimicrobial therapies of the future.

MATERIALS AND METHODS

Bacterial strains, CP purification, and culturing. *H. pylori* strains G27 and 7.13 (B128 derivative) were used for these studies. *H. pylori* strains were cultured on tryptic soy agar plates supplemented with 5% sheep blood or in brucella broth supplemented with 10% fetal bovine serum (FBS) at 37°C in room air supplemented with 5% CO₂. Purification of calprotectin was performed, as previously described (28). *H. pylori* strains G27 and 7.13 with mutations in *lpxF*, *lpxL*, or *lpxR* were generated using constructs provided by the Trent laboratory, as previously described (23, 48).

Growth curve analyses. For bacterial growth assays, *H. pylori* strains were grown under shaking conditions in 60% brucella broth plus 40% calprotectin buffer (28) supplemented with 10% FBS alone or supplemented with 100 μM Zn chloride and/or 100 μM Mn chloride, with increasing concentrations of CP at 37°C in room air supplemented with 5% CO₂. Bacterial growth was measured using a spectrophotometric reading (optical density) at 600 nm (OD₆₀₀). Pretreatment assays were performed by exposing *H. pylori* to subinhibitory concentrations of CP (100 μg/ml) for 24 h prior to 1:10 dilution subculture and exposure to increasing concentrations of CP alone or in the presence of an exogenous nutrient metal source (Zn/Mn).

Inductively coupled plasma mass spectrometry. Bacterial cells were grown in 60% brucella broth plus 40% calprotectin buffer (28) supplemented with 10% FBS alone or with 200 $\mu\text{g}/\text{ml}$ CP, or CP plus 100 μM exogenous metal (zinc chloride or manganese chloride) for 24 h, with shaking, at 37°C in room air supplemented with 5% CO_2 . Cells were pelleted at $4,000 \times g$ for 15 min before washing once with 0.5 M EDTA and three times with 5 ml of distilled water. Samples were weighed and digested in 1 ml of 50% nitric acid overnight at 50°C. Elemental quantification was performed using a Thermo-Element 2 HR-ICPMS apparatus (Thermo, Fisher Scientific, Bremen, Germany), as previously described (30).

Biofilm assays. *H. pylori* biofilms were grown in 3-ml polystyrene tubes (under static conditions) in 60% brucella broth plus 40% calprotectin buffer (28) supplemented with 10% FBS alone or with 200 $\mu\text{g}/\text{ml}$ CP, or CP plus 100 μM exogenous metal for 2 to 4 days at 37°C in room air supplemented with 5% CO_2 . After biofilms were formed, they were quantitatively analyzed, as previously described (40), by measuring the OD_{600} , staining the biofilm with crystal violet, and resolubilizing the crystal violet in 80% ethanol–20% acetone solution before measuring the absorbance (OD) at 540 nm. The ratio of total biofilm to biomass was calculated via the formula $\text{OD}_{540}/\text{OD}_{600}$.

BATH assay. Cell surface hydrophobicity can be determined via a BATH assay, which measures the percentage of bacterial cells that are associated with the xylene fraction as a measure of hydrophobicity. The *H. pylori* biofilm was scraped and resuspended in 1.2 ml PUM buffer (phosphate, urea, and magnesium sulfate; 0.1 M $\text{K}_2\text{HPO}_4 \cdot 3\text{H}_2\text{O}$, 50 mM KH_2PO_4 , 30 mM urea, 0.5 M $\text{MgSO}_4 \cdot 7\text{H}_2\text{O}$; pH 7.10), and the bacterial density was obtained by measuring the absorbance (OD) at 540 nm. Two hundred microliters of xylene was then added, and the sample was vortexed vigorously and allowed to separate into aqueous and hydrocarbon fractions. The aqueous fraction was carefully pipetted out, and the bacterial density was measured spectrophotometrically. The percent cell surface hydrophobicity was determined using the following equation: $\{(A_{540} \text{ before xylene addition}) - (A_{540} \text{ after xylene addition})\} / (A_{540} \text{ before xylene addition}) \times 100$, as previously described (41).

Field emission gun scanning electron microscopy of biofilms. *H. pylori* biofilms were imaged by FEG-SEM analysis using methods previously described (40). Briefly, *H. pylori* biofilms were grown on polystyrene for 48 h at 37°C in the presence of 5% CO_2 . Cells were fixed with 2.0% paraformaldehyde–2.5% glutaraldehyde in 0.05 M sodium cacodylic acid buffer for 1 h at room temperature. Samples were washed three times with cacodylic acid buffer before sequential dehydration with increasing concentrations of ethanol. Samples were then dried at the critical point, mounted onto SEM stubs, painted with colloidal silver at the sample edge, and sputter coated with 20-nm-diameter gold-palladium. Samples were visualized with an FEI Quanta 250 FEG-SEM apparatus under high vacuum pressure, and micrographs were analyzed with ImageJ software.

Confocal laser scanning microscopy. *H. pylori* biofilms were grown on plastic coverslips as described above, washed three times with $1 \times$ phosphate-buffered saline (PBS) and placed in 1 ml PBS before staining with the Live/Dead BacLight kit (Life Technologies), which is comprised of SYTO 9 (green) and propidium iodide (red) and entails counterstaining with calcofluor white (blue; Sigma Aldrich). Biofilms were stained with 6 μl of 1.67 mM SYTO 9 and 1.67 mM propidium iodide mixture, and counterstained with 6 μl of 10-mg/ml calcofluor white solution for 1 h; the biofilms were washed three times with $1 \times$ PBS and mounted onto coverslips with ProLong gold antifade reagent (Life Technologies). Samples were imaged with a Zeiss 710 confocal laser scanning microscope and analyzed using Zen software.

Purification and analysis of lipid A. *H. pylori* lipid A extraction was carried out by mild acid hydrolysis as previously described (23, 78). For mass spectrometry, lipid A was analyzed using a MALDI-TOF/TOF (ABI 4700 Proteomics analyzer) mass spectrometer in the negative mode, as previously described (23, 78).

RNA isolation and analysis of gene expression by real-time PCR. Total RNA was isolated from *H. pylori* using by using Tri reagent solution (Ambion) according to the manufacturer's instructions, with slight modifications. Bacterial pellets were resuspended in Tri reagent solution, and one chloroform extraction was performed. The RNA was then mixed with 70% ethanol and purified using the RNeasy minikit (Qiagen). RNA samples were DNase treated using DNA-free DNase (Ambion). RNA was then reverse transcribed using the high-capacity RNA-to-cDNA kit (Applied Biosystems). As a control, samples were processed without reverse transcriptase. The cDNA and control reaction mixtures were diluted 1:10 and used in real-time PCRs. Real-time PCR was performed using a Step one Plus real-time PCR machine (Applied Biosystems), with SYBR green as the fluorochrome. Abundance of transcript was calculated using the $\Delta\Delta\text{CT}$ method, with each transcript signal normalized to the abundance of the 16S rRNA internal control. The normalized transcript signal for each sample was then compared to similarly normalized values obtained with bacteria grown *in vitro* or under control conditions. Primer sequences are as follows: *lpxI* forward, 5' TATGAGTAGGCGAGAGGGCT 3'; *lpxI* reverse, 5' GTAGCGGCGGATAAAAATAG 3'; *lpxF* forward, 5' CCCTACGGCTTGCAAAAATAA 3'; *lpxF* reverse, 5' GGGCTTGGGATCTTTCCTTC 3'; *lpxR* forward, 5' TTGCATGACAACCACCCCTTA 3'; *lpxR* reverse, 5' GCGTGTTCAGCCATAAAAAT 3'.

Statistical analysis. Statistical analyses of bacterial growth, BATH assay results, polymyxin MICs, and quantitative biofilm assays were performed using one-way analysis of variance (ANOVA) with Tukey's correction for multiple comparisons, or a paired two-tailed Student's *t* test. All data were derived from at least three separate biological replicates unless specified otherwise. Statistical analyses were performed using GraphPad Prism software.

SUPPLEMENTAL MATERIAL

Supplemental material for this article may be found at <http://mbio.asm.org/lookup/suppl/doi:10.1128/mBio.01349-15/-/DCSupplemental>.

- Figure S1, PDF file, 0.1 MB.
- Figure S2, PDF file, 0.2 MB.
- Figure S3, PDF file, 0.03 MB.
- Figure S4, PDF file, 0.3 MB.
- Table S1, PDF file, 0.3 MB.

ACKNOWLEDGMENTS

Core services were performed through Vanderbilt University Medical Center's Digestive Disease Research Center, which is supported by NIH Core Scholarship grant P30DK058404.

Experiments were performed in part through the use of the Vanderbilt University Medical Center Cell Imaging Shared Resource.

REFERENCES

1. Mane SP, Dominguez-Bello MG, Blaser MJ, Sobral BW, Hontecillas R, Skoneczka J, Mohapatra SK, Crasta OR, Evans C, Modise T, Shallom S, Shukla M, Varon C, Megraud F, Maldonado-Contreras AL, Williams KP, Bassaganya-Riera J. 2010. Host-interactive genes in Amerindian *Helicobacter pylori* diverge from their Old World homologs and mediate inflammatory responses. *J Bacteriol* 192:3078–3092. <http://dx.doi.org/10.1128/JB.00063-10>.
2. Bik EM, Eckburg PB, Gill SR, Nelson KE, Purdom EA, Francois F, Perez-Perez G, Blaser MJ, Relman DA. 2006. Molecular analysis of the bacterial microbiota in the human stomach. *Proc Natl Acad Sci U S A* 103:732–737. <http://dx.doi.org/10.1073/pnas.0506655103>.
3. Ghose C, Perez-Perez GI, van Doorn LJ, Dominguez-Bello MG, Blaser MJ. 2005. High frequency of gastric colonization with multiple *Helicobacter pylori* strains in Venezuelan subjects. *J Clin Microbiol* 43:2635–2641. <http://dx.doi.org/10.1128/JCM.43.6.2635-2641.2005>.
4. Noto JM, Peek RM, Jr. 2012. *Helicobacter pylori*: an overview. *Methods Mol Biol* 921:7–10. http://dx.doi.org/10.1007/978-1-62703-005-2_2.
5. Bauer B, Meyer TF. 2011. The human gastric pathogen *Helicobacter pylori* and its association with gastric cancer and ulcer disease. *Ulcer* 2011: 340157. <http://dx.doi.org/10.1155/2011/340157>.
6. Algood HM, Gallo-Romero J, Wilson KT, Peek RM, Jr, Cover TL. 2007.

- Host response to *Helicobacter pylori* infection before initiation of the adaptive immune response. *FEMS Immunol Med Microbiol* 51:577–586. <http://dx.doi.org/10.1111/j.1574-695X.2007.00338.x>.
7. Wilson KT, Crabtree JE. 2007. Immunology of *Helicobacter pylori*: insights into the failure of the immune response and perspectives on vaccine studies. *Gastroenterology* 133:288–308. <http://dx.doi.org/10.1053/j.gastro.2007.05.008>.
 8. Karttunen R, Karttunen T, Ekre HP, MacDonald TT. 1995. Interferon gamma and interleukin 4 secreting cells in the gastric antrum in *Helicobacter pylori* positive and negative gastritis. *Gut* 36:341–345. <http://dx.doi.org/10.1136/gut.36.3.341>.
 9. Haerberle HA, Kubin M, Bamford KB, Garofalo R, Graham DY, El-Zaatari F, Karttunen R, Crowe SE, Reyes VE, Ernst PB. 1997. Differential stimulation of interleukin-12 (IL-12) and IL-10 by live and killed *Helicobacter pylori* in vitro and association of IL-12 production with gamma interferon-producing T cells in the human gastric mucosa. *Infect Immun* 65:4229–4235.
 10. Bamford KB, Fan X, Crowe SE, Leary JF, Gourley WK, Luthra GK, Brooks EG, Graham DY, Reyes VE, Ernst PB. 1998. Lymphocytes in the human gastric mucosa during *Helicobacter pylori* have a T helper cell 1 phenotype. *Gastroenterology* 114:482–492. [http://dx.doi.org/10.1016/S0016-5085\(98\)70531-1](http://dx.doi.org/10.1016/S0016-5085(98)70531-1).
 11. Lindholm C, Quiding-Jarbrink M, Lonroth H, Hamlet A, Svennerholm AM. 1998. Local cytokine response in *Helicobacter pylori*-infected subjects. *Infect Immun* 66:5964–5971.
 12. Sommer F, Faller G, Konturek P, Kirchner T, Hahn EG, Zeus J, Rollinghoff M, Lohoff M. 1998. Antrum- and corpus mucosa-infiltrating CD4⁺ lymphocytes in *Helicobacter pylori* gastritis display a Th1 phenotype. *Infect Immun* 66:5543–5546.
 13. Luzzza F, Parrello T, Sebko L, Pensabene L, Imeneo M, Mancuso M, La Vecchia AM, Monteleone G, Strisciuglio P, Pallone F. 2001. Expression of proinflammatory and Th1 but not Th2 cytokines is enhanced in gastric mucosa of *Helicobacter pylori* infected children. *Dig Liver Dis* 33:14–20. [http://dx.doi.org/10.1016/S1590-8658\(01\)80130-4](http://dx.doi.org/10.1016/S1590-8658(01)80130-4).
 14. Itoh T, Yoshida M, Chiba T, Kita T, Wakatsuki Y. 2003. A coordinated cytotoxic effect of IFN-gamma and cross-reactive antibodies in the pathogenesis of *Helicobacter pylori* gastritis. *Helicobacter* 8:268–278. <http://dx.doi.org/10.1046/j.1523-5378.2003.00154.x>.
 15. Mizuno T, Ando T, Nobata K, Tsuzuki T, Maeda O, Watanabe O, Minami M, Ina K, Kusugami K, Peek RM, Goto H. 2005. Interleukin-17 levels in *Helicobacter pylori*-infected gastric mucosa and pathologic sequelae of colonization. *World J Gastroenterol* 11:6305–6311. <http://dx.doi.org/10.3748/wjg.v11.i40.6305>.
 16. Caruso R, Fina D, Paoluzi O, Del Vecchio Blanco G, Stolfi C, Rizzo A, Caprioli F, Sarra M, Andrei F, Fantini M, MacDonald T, Pallone F, Monteleone G. 2008. IL-23-mediated regulation of IL-17 production in *Helicobacter pylori*-infected gastric mucosa. *Eur J Immunol* 38:470–478. <http://dx.doi.org/10.1002/eji.200737635>.
 17. Sugimoto M, Ohno T, Graham DY, Yamaoka Y. 2009. Gastric mucosal interleukin-17 and -18 mRNA expression in *Helicobacter pylori*-induced Mongolian gerbils. *Cancer Sci* 100:2152–2159. <http://dx.doi.org/10.1111/j.1349-7006.2009.01291.x>.
 18. Horvath DJ, Jr, Washington MK, Cope VA, Algood HM. 2012. IL-23 contributes to control of chronic *Helicobacter pylori* infection and the development of T helper responses in a mouse model. *Front Immunol* 3:56. <http://dx.doi.org/10.3389/fimmu.2012.00056>.
 19. Herrera CM, Crofts AA, Henderson JC, Pingali SC, Davies BW, Trent MS. 2014. The *Vibrio cholerae* VprA-VprB two-component system controls virulence through endotoxin modification. *mBio* 5:e02283-14. <http://dx.doi.org/10.1128/mBio.02283-14>.
 20. Shah NR, Hancock REW, Fernandez RC. 2014. *Bordetella pertussis* lipid A glucosamine modification confers resistance to cationic antimicrobial peptides and increases resistance to outer membrane perturbation. *Antimicrob Agents Chemother* 58:4931–4934. <http://dx.doi.org/10.1128/AAC.02590-14>.
 21. Rolin O, Muse SJ, Safi C, Elahi S, Gerds V, Hittle LE, Ernst RK, Harvill ET, Preston A, Pirofski L. 2014. Enzymatic modification of lipid A by ArnT protects *Bordetella bronchiseptica* against cationic peptides and is required for transmission. *Infect Immun* 82:491–499. <http://dx.doi.org/10.1128/IAI.01260-12>.
 22. Olaitan AO, Morand S, Rolain J. 2014. Mechanisms of polymyxin resistance: acquired and intrinsic resistance in bacteria. *Front Microbiol* 5:643. <http://dx.doi.org/10.3389/fmicb.2014.00643>.
 23. Cullen TW, Giles DK, Wolf LN, Ecobichon C, Boneca IG, Trent MS. 2011. *Helicobacter pylori* versus the host: remodeling of the bacterial outer membrane is required for survival in the gastric mucosa. *PLoS Pathog* 7:e1002454. <http://dx.doi.org/10.1371/journal.ppat.1002454>.
 24. Gebhardt C, Németh J, Angel P, Hess J. 2006. S100A8 and S100A9 in inflammation and cancer. *Biochem Pharmacol* 72:1622–1631. <http://dx.doi.org/10.1016/j.bcp.2006.05.017>.
 25. Urban CF, Ermert D, Schmid M, Abu-Abed U, Goosmann C, Nacken W, Brinkmann V, Jungblut PR, Zychlinsky A. 2009. Neutrophil extracellular traps contain calprotectin, a cytosolic protein complex involved in host defense against *Candida albicans*. *PLoS Pathog* 5:e1000639. <http://dx.doi.org/10.1371/journal.ppat.1000639>.
 26. Hood MI, Skaar EP. 2012. Nutritional immunity: transition metals at the pathogen-host interface. *Nat Rev Microbiol* 10:525–537. <http://dx.doi.org/10.1038/nrmicro2836>.
 27. Damo SM, Kehl-Fie TE, Sugitani N, Holt ME, Rathi S, Murphy WJ, Zhang Y, Betz C, Hench L, Fritz G, Skaar EP, Chazin WJ. 2013. Molecular basis for manganese sequestration by calprotectin and roles in the innate immune response to invading bacterial pathogens. *Proc Natl Acad Sci U S A* 110:3841–3846. <http://dx.doi.org/10.1073/pnas.1220341110>.
 28. Kehl-Fie T, Chitayat S, Hood M, Damo S, Restrepo N, Garcia C, Munro K, Chazin W, Skaar E. 2011. Nutrient metal sequestration by calprotectin inhibits bacterial superoxide defense, enhancing neutrophil killing of *Staphylococcus aureus*. *Cell Host Microbe* 10:158–164. <http://dx.doi.org/10.1016/j.chom.2011.07.004>.
 29. Corbin BD, Seeley EH, Raab A, Feldmann J, Miller MR, Torres VJ, Anderson KL, Dattilo BM, Dunman PM, Gerads R, Caprioli RM, Nacken W, Chazin WJ, Skaar EP. 2008. Metal chelation and inhibition of bacterial growth in tissue abscesses. *Science* 319:962–965. <http://dx.doi.org/10.1126/science.1152449>.
 30. Hood MI, Mortensen BL, Moore JL, Zhang Y, Kehl-Fie TE, Sugitani N, Chazin WJ, Caprioli RM, Skaar EP. 2012. Identification of an *Acinetobacter baumannii* zinc acquisition system that facilitates resistance to calprotectin-mediated zinc sequestration. *PLoS Pathog* 8:e1003068. <http://dx.doi.org/10.1371/journal.ppat.1003068>.
 31. Liu J, Jellbauer S, Poe AJ, Ton V, Pesciaroli M, Kehl-Fie TE, Restrepo N, Hosking MP, Edwards R, Battistoni A, Pasquali P, Lane T, Chazin W, Vogl T, Roth J, Skaar E, Raffatellu M. 2012. Zinc sequestration by the neutrophil protein calprotectin enhances *Salmonella* growth in the inflamed gut. *Cell Host Microbe* 11:227–239. <http://dx.doi.org/10.1016/j.chom.2012.01.017>.
 32. Loomans H, Hahn B, Li Q, Phadnis S, Sohnle P. 1998. Histidine-based zinc-binding sequences and the antimicrobial activity of calprotectin. *J Infect Dis* 177:812–814. <http://dx.doi.org/10.1086/517816>.
 33. Lusitani D, Malawista SE, Montgomery RR. 2003. Calprotectin, an abundant cytosolic protein from human polymorphonuclear leukocytes, inhibits the growth of *Borrelia burgdorferi*. *Infect Immun* 71:4711–4716. <http://dx.doi.org/10.1128/IAI.71.8.4711-4716.2003>.
 34. Sohnle P, Hunter M, Hahn B, Chazin W. 2000. Zinc-reversible antimicrobial activity of recombinant calprotectin (migration inhibitory factor-related proteins 8 and 14). *J Infect Dis* 182:1272–1275. <http://dx.doi.org/10.1086/315810>.
 35. Steinbakk M, Naess-Andresen CF, Lingaas E, Dale I, Brandtzaeg P, Fagerhol MK. 1990. Antimicrobial actions of calcium binding leucocyte L1 protein, calprotectin. *Lancet* 336:763–765. [http://dx.doi.org/10.1016/0140-6736\(90\)93237-J](http://dx.doi.org/10.1016/0140-6736(90)93237-J).
 36. Zaia AA, Sappington KJ, Nisapakultorn K, Chazin WJ, Dietrich EA, Ross KF, Herzberg MC. 2009. Subversion of antimicrobial calprotectin (S100A8/S100A9 complex) in the cytoplasm of TR146 epithelial cells after invasion by *Listeria monocytogenes*. *Mucosal Immunol* 2:43–53. <http://dx.doi.org/10.1038/mi.2008.63>.
 37. Gaddy JA, Radin JN, Loh JT, Piazuolo MB, Kehl-Fie TE, Delgado AG, Ica FT, Peek RM, Cover TL, Chazin WJ, Skaar EP, Algood HMS. 2014. The host protein calprotectin modulates the *Helicobacter pylori* cag type IV secretion system via zinc sequestration. *PLoS Pathog* 10:e1004450. <http://dx.doi.org/10.1371/journal.ppat.1004450>.
 38. Raffatellu M, George MD, Akiyama Y, Hornsby MJ, Nuccio S, Paixao TA, Butler BP, Chu H, Santos RL, Berger T, Mak TW, Tsolis RM, Bevins CL, Solnick JV, Dandekar S, Bäumlner AJ. 2009. Lipocalin-2 resistance confers an Advantage to *Salmonella enterica* serotype Typhimurium for growth and survival in the inflamed intestine. *Cell Host Microbe* 5:476–486. <http://dx.doi.org/10.1016/j.chom.2009.03.011>.

39. Diaz-Ochoa VE, Jellbauer S, Klaus S, Raffatellu M. 2014. Transition metal ions at the crossroads of mucosal immunity and microbial pathogenesis. *Front Cell Infect Microbiol* 4:2. <http://dx.doi.org/10.3389/fcimb.2014.00002>.
40. Gaddy JA, Tomaras AP, Actis LA. 2009. The *Acinetobacter baumannii* 19606 OmpA protein plays a role in biofilm formation on abiotic surfaces and in the interaction of this pathogen with eukaryotic cells. *Infect Immun* 77:3150–3160. <http://dx.doi.org/10.1128/IAI.00096-09>.
41. Brossard KA, Campagnari AA. 2012. The *Acinetobacter baumannii* biofilm-associated protein plays a role in adherence to human epithelial cells. *Infect Immun* 80:228–233. <http://dx.doi.org/10.1128/IAI.05913-11>.
42. Andersen LP, Rasmussen L. 2009. *Helicobacter pylori*: coccoid forms and biofilm formation. *FEMS Immunol Med Microbiol* 56:112–115. <http://dx.doi.org/10.1111/j.1574-695X.2009.00556.x>.
43. Chan ACK, Blair KM, Liu Y, Frirdich E, Gaynor EC, Tanner ME, Salama NR, Murphy MEP. 2015. Helical shape of *Helicobacter pylori* requires an atypical glutamine as a zinc ligand in the carboxypeptidase Csd4. *J Biol Chem* 290:3622–3638. <http://dx.doi.org/10.1074/jbc.M114.624734>.
44. Carron M, Tran V, Sugawa C, Coticchia J. 2006. Identification of *Helicobacter pylori* biofilms in human gastric mucosa. *J Gastrointest Surg* 10:712–717. <http://dx.doi.org/10.1016/j.gassur.2005.10.019>.
45. Kato A, Chen H, Latifi T, Groisman E. 2012. Reciprocal control between a bacterium's regulatory system and the modification status of its lipopolysaccharide. *Mol Cell* 47:897–908. <http://dx.doi.org/10.1016/j.molcel.2012.07.017>.
46. Leptihn S, Har JY, Wohland T, Ding JL. 2010. Correlation of charge, hydrophobicity, and structure with antimicrobial activity of S1 and Miriam peptides. *Biochemistry* 49:9161–9170. <http://dx.doi.org/10.1021/bi1011578>.
47. Stead C, Tran A, Ferguson D, Jr., McGrath S, Cotter R, Trent S. 2005. A novel 3-deoxy-D-manno-octulosonic acid (Kdo) hydrolase that removes the outer Kdo sugar of *Helicobacter pylori* lipopolysaccharide. *J Bacteriol* 187:3374–3383. <http://dx.doi.org/10.1128/JB.187.10.3374-3383.2005>.
48. Stead CM, Beasley A, Cotter RJ, Trent MS. 2008. Deciphering the unusual acylation pattern of *Helicobacter pylori* lipid A. *J Bacteriol* 190:7012–7021. <http://dx.doi.org/10.1128/JB.00667-08>.
49. Stead CM, Zhao J, Raetz CRH, Trent MS. 2010. Removal of the outer Kdo from *Helicobacter pylori* lipopolysaccharide and its impact on the bacterial surface. *Mol Microbiol* 78:837–852. <http://dx.doi.org/10.1111/j.1365-2958.2010.07304.x>.
50. Tran AX, Karbarz MJ, Wang X, Raetz CRH, McGrath SC, Cotter RJ, Trent MS. 2004. Periplasmic cleavage and modification of the 1-phosphate group of *Helicobacter pylori* lipid A. *J Biol Chem* 279:55780–55791. <http://dx.doi.org/10.1074/jbc.M406480200>.
51. Chalabaev S, Chauhan A, Novikov A, Iyer P, Szczesny M, Beloin C, Carolf M, Ghigo JM. 2014. Biofilms formed by gram-negative bacteria undergo increased lipid A palmitoylation, enhancing *in vivo* survival. *mBio* 5:e01116-14. <http://dx.doi.org/10.1128/mBio.01116-14>.
52. Cullen TW, Schofield WB, Barry NA, Putnam EE, Rundell EA, Trent MS, Degan PH, Booth CJ, Yu H, Goodman AL. 2015. Gut microbiota. Antimicrobial peptide resistance mediates resilience of prominent gut commensals during inflammation. *Science* 347:170–175. <http://dx.doi.org/10.1126/science.1260580>.
53. Clohessy PA, Golden BE. 1995. Calprotectin-mediated zinc chelation as a biostatic mechanism in host defence. *Scand J Immunol* 42:551–556. <http://dx.doi.org/10.1111/j.1365-3083.1995.tb03695.x>.
54. Vigneshkumar B, Radhakrishnan S, Balamurugan K. 2014. Analysis of *Pseudomonas aeruginosa* PAO1 lipid A changes during the interaction with model organism, *Caenorhabditis elegans*. *Lipids* 49:555–575. <http://dx.doi.org/10.1007/s11745-014-3898-3>.
55. Vanderlinde EM, Muszynski A, Harrison JJ, Koval SF, Foreman DL, Ceri H, Kannenberg EL, Carlson RW, Yost CK. 2009. *Rhizobium leguminosarum* biovar viciae 3841, deficient in 27-hydroxyoctacosanoate-modified lipopolysaccharide, is impaired in desiccation tolerance, biofilm formation and motility. *Microbiology* 155:3055–3069. <http://dx.doi.org/10.1099/mic.0.025031-0>.
56. Cole KE, Gattis SG, Angell HD, Fierke CA, Christianson DW. 2011. Structure of the metal-dependent deacetylase LpxC from *Yersinia enterocolitica* complexed with the potent inhibitor CHIR-090. *Biochemistry* 50:258–265. <http://dx.doi.org/10.1021/bi101622a>.
57. Barb AW, Zhou P. 2008. Mechanism and inhibition of LpxC: an essential zinc-dependent deacetylase of bacterial lipid A synthesis. *Curr Pharm Biotechnol* 9:9–15. <http://dx.doi.org/10.2174/138920108783497668>.
58. Jackman JE, Raetz CRH, Fierke CA. 1999. UDP-3-O-(R-3-hydroxymyristoyl)-N-acetylglucosamine deacetylase of *Escherichia coli* is a zinc metalloenzyme. *Biochemistry* 38:1902–1911. <http://dx.doi.org/10.1021/bi982339s>.
59. McClerren AL, Endsley S, Bowman JL, Andersen NH, Guan Z, Rudolph J, Raetz CRH. 2005. A slow, tight-binding inhibitor of the zinc-dependent deacetylase LpxC of lipid A biosynthesis with antibiotic activity comparable to ciprofloxacin. *Biochemistry* 44:16574–16583. <http://dx.doi.org/10.1021/bi0518186>.
60. Nowicki EM, O'Brien JP, Brodbelt JS, Trent MS. 2015. Extracellular zinc induces phosphoethanolamine addition to *Pseudomonas aeruginosa* lipid A via the ColRS two-component system. *Mol Microbiol* 97:166–178. <http://dx.doi.org/10.1111/mmi.13018>.
61. Rutten L, Mannie JBA, Stead CM, Raetz CRH, Reynolds CM, Bonvin AMJJ, Tommassen JP, Egmond MR, Trent MS, Gros P. 2009. Active-site architecture and catalytic mechanism of the lipid A deacetylase LpxR of *Salmonella typhimurium*. *Proc Natl Acad Sci U S A* 106:1960–1964. <http://dx.doi.org/10.1073/pnas.0813064106>.
62. Reynolds CM, Ribeiro AA, McGrath SC, Cotter RJ, Raetz CR, Trent MS. 2006. An outer membrane enzyme encoded by *Salmonella typhimurium* lpxR that removes the 3'-acyloxyacyl moiety of lipid A. *J Biol Chem* 281:21974–21987. <http://dx.doi.org/10.1074/jbc.M603527200>.
63. Costerton JW, Stewart PS, Greenberg EP. 1999. Bacterial biofilms: a common cause of persistent infections. *Science* 284:1318–1322. <http://dx.doi.org/10.1126/science.284.5418.1318>.
64. Donlan RM, Costerton JW. 2002. Biofilms: survival mechanisms of clinically relevant microorganisms. *Clin Microbiol Rev* 15:167–193. <http://dx.doi.org/10.1128/CMR.15.2.167-193.2002>.
65. Vuong C, Voyich JM, Fischer ER, Braughton KR, Whitney AR, DeLeo FR, Otto M. 2004. Polysaccharide intercellular adhesin (PIA) protects *Staphylococcus epidermidis* against major components of the human innate immune system. *Cell Microbiol* 6:269–275. <http://dx.doi.org/10.1046/j.1462-5822.2004.00367.x>.
66. Fong JCN, Yildiz FH. 2008. Interplay between cyclic AMP-cyclic AMP receptor protein and cyclic di-GMP signaling in *Vibrio cholerae* biofilm formation. *J Bacteriol* 190:6646–6659. <http://dx.doi.org/10.1128/JB.00466-08>.
67. Hinnebusch BJ, Erickson DL. 2008. *Yersinia pestis* biofilm in the flea vector and its role in the transmission of plague. *Curr Top Microbiol Immunol* 322:229–248. http://dx.doi.org/10.1007/978-3-540-75418-3_11.
68. Borlee BR, Goldman AD, Murakami K, Samudrala R, Wozniak DJ, Parsek MR. 2010. *Pseudomonas aeruginosa* uses a cyclic-di-GMP-regulated adhesion to reinforce the biofilm extracellular matrix. *Mol Microbiol* 75:827–842. <http://dx.doi.org/10.1111/j.1365-2958.2009.06991.x>.
69. Yang F, Hassambhai AM, Chen H, Huang Z, Lin T, Wu S, Ho B. 2011. Proteomannans in biofilm of *Helicobacter pylori* ATCC 43504. *Helicobacter* 16:89–98. <http://dx.doi.org/10.1111/j.1523-5378.2010.00815.x>.
70. Grande R, Di Giulio M, Bessa LJ, Di Campli E, Baffoni M, Guarnieri S, Cellini L. 2011. Extracellular DNA in *Helicobacter pylori* biofilm: a backstairs rumour. *J Appl Microbiol* 110:490–498. <http://dx.doi.org/10.1111/j.1365-2672.2010.04911.x>.
71. Yonezawa H, Osaki T, Kurata S, Fukuda M, Kawakami H, Ochiai K, Hanawa T, Kamiya S. 2009. Outer membrane vesicles of *Helicobacter pylori* TK1402 are involved in biofilm formation. *BMC Microbiol* 9:197. <http://dx.doi.org/10.1186/1471-2180-9-197>.
72. Mah TC, O'Toole GA. 2001. Mechanisms of biofilm resistance to antimicrobial agents. *Trends Microbiol* 9:34–39. [http://dx.doi.org/10.1016/S0966-842X\(00\)01913-2](http://dx.doi.org/10.1016/S0966-842X(00)01913-2).
73. Hsu C, Lin M, Chen C, Chien S, Cheng Y, Su I, Shu J. 2011. Vancomycin promotes the bacterial autolysis, release of extracellular DNA, and biofilm formation in vancomycin-non-susceptible *Staphylococcus aureus*. *FEMS Immunol Med Microbiol* 63:236–247. <http://dx.doi.org/10.1111/j.1574-695X.2011.00846.x>.
74. Berlutti F, Ajello M, Bosso P, Morea C, Petrucca A, Antonini G, Valenti P. 2004. Both lactoferrin and iron influence aggregation and biofilm formation in *Streptococcus mutans*. *Biomaterials* 25:271–278. <http://dx.doi.org/10.1023/B:BIOM.0000027704.53859.d3>.
75. Morita Y, Tomida J, Kawamura Y. 2014. Responses of *Pseudomonas aeruginosa* to antimicrobials. *Front Microbiol* 4:422. <http://dx.doi.org/10.3389/fmicb.2013.00422>.

76. Malcolm J, Sherriff A, Lappin DF, Ramage G, Conway DI, Macpherson LMD, Culshaw S. 2014. Salivary antimicrobial proteins associate with age-related changes in streptococcal composition in dental plaque. *Mol Oral Microbiol* 29:284–293. <http://dx.doi.org/10.1111/omi.12058>.
77. Bessa LJ, Grande R, Di Iorio DD, Di Giulio MD, Di Campli ED, Cellini L. 2013. *Helicobacter pylori* free-living and biofilm modes of growth: behavior in response to different culture media. *APMIS* 121:549–560. <http://dx.doi.org/10.1111/apm.12020>.
78. Tran AX, Whittimore JD, Wyrick PB, McGrath SC, Cotter RJ, Trent MS. 2006. The lipid A 1-phosphatase of *Helicobacter pylori* is required for resistance to the antimicrobial peptide polymyxin. *J Bacteriol* 188: 4531–4541. <http://dx.doi.org/10.1128/JB.00146-06>.